GA–A26319

PHYSICS AND ENGINEERING ISSUES ASSOCIATED WITH EDGE LOCALIZED MODE CONTROL IN ITER

by
M.R. WADE

DECEMBER 2008

GENERAL ATOMICS

DISCLAIMER

GA–A26319

PHYSICS AND ENGINEERING ISSUES ASSOCIATED WITH EDGE LOCALIZED MODE CONTROL IN ITER

by
M.R. WADE

This is a preprint of an invited paper presented at the Twenty-Fifth Symposium on Fusion Technology, September 15-19, 2008, in Rostock, Germany, and to be published in *Fusion Engineering and Design*.

Work supported in part by
the U.S. Department of Energy
under DE-FC02-04ER54698

GENERAL ATOMICS PROJECT 30200
DECEMBER 2008

ABSTRACT

The mitigation or suppression of large edge localized modes (ELMs) is a critical issue for successful operation of ITER. In recent years, a concerted worldwide effort has emerged to develop efficient and reliable ELM mitigation and suppression techniques that can be scaled to the full range of ITER regimes and more generally to burning plasmas in a generic fusion reactor design. These techniques include the use of small-ELM or ELM-free regimes, the repetitive triggering of ELMs by external means, and the suppression of ELMs with non-axisymmetric fields. The extrapolation of all of these techniques to ITER is highly uncertain due to outstanding physics issues. However, two techniques have emerged as the preferred methods for use in ITER: ELM pacing using pellet injection and the use of edge resonant magnetic perturbations for ELM suppression. This paper discusses the issues related to ELM control in ITER, provides a general introduction to various ELM control techniques, and a more detailed discussion of the physics and engineering requirements of the two preferred techniques for ELM control in ITER.

1 INTRODUCTION

The control of edge instabilities known as edge localized modes (ELMs) has been identified as a critical issue for ITER in maximizing the lifetime of divertor plasma facing components. ELMs are a ubiquitous feature of the H-mode confinement regime, which is projected to be necessary for ITER to achieve $Q = 10$ (Q is the ratio of self-generated fusion power to the input power) [1]. This regime is characterized by an edge transport barrier that leads to the build-up of a large pressure gradient in this region, eventually leading to destabilization of an MHD instability that causes rapid ($\sim$100 μs) transport of heat and particles into the open field-line region ([2],[3],[4]). These so-called ELMs are projected (if not mitigated) to produce energy bursts that result in impulsive energy densities on the divertor target plate that are well above the ablative limits of plasma facing material envisioned for ITER, leading to premature erosion of the divertor target plates and frequent replacement of divertor components.

In recent years, a concerted worldwide effort has emerged to develop efficient and reliable ELM mitigation techniques that can be scaled to the full range of ITER regimes and more generally to burning plasmas in a generic fusion reactor design. Type I ELMs are believed to pose the most serious concern for ITER. Substantial experimental and theoretical evidence suggests that these ELMs are ideal MHD instabilities of moderate toroidal mode number ($n = 5 - 15$) and spatial extent ($\Delta\rho \simeq 0.1$ where ρ is the normalized minor radius) that are driven unstable by both the edge pressure gradient and edge current density [5]. Various techniques have been developed to varying degrees of maturity for this purpose. These techniques can be broadly characterized in three categories: 1) operating regimes without ELMs or with significantly reduced ELM size; 2) methods that trigger ELMs of smaller size than would naturally occur otherwise and 3) methods for altering the edge transport (and associated pressure gradient) to avoid triggering of an ELM altogether. At present, the ITER design envisions two primary ELM control techniques: ELM pacing using pellet injection and ELM mitigation/suppression using resonant magnetic perturbations (RMPs) at the plasma edge [6].

A brief introduction of the requirements for ELM control in ITER are presented in Section 2. In Section 3, the basic concepts, issues, and limitations associated with potential approaches will be briefly reviewed. In Section 4, more detailed information will be provided on the various design and physics issues associated with the two presently planned approaches in ITER: ELM pacing by pellet injection and ELM mitigation using RMPs at the plasma edge. In particular, we will discuss the delivery requirements (penetration and rate) for pellet pacing to be successful and the implications of these requirements on plasma performance. Several potential RMP coil designs that have been considered during the design review process and how these design variations are expected to affect various aspects of RMP H-mode performance will be described.

2 ELM CONTROL REQUIREMENTS FOR ITER

Unmitigated ELMs at the full plasma current ($I_p = 15$ MA) of ITER are anticipated to expel nearly 10% of the pedestal energy on a very short time scale. ELMs of this size, anticipated to occur every second, would result in incident energy densities on the divertor target plates approaching 10 MJ/m^2 [6]. Recent studies of candidate materials for ITER indicate that the tolerable pulsed energy density in ITER is approximately 0.5 MJ/m^2 for both tungsten and carbon fiber composite components [7]. Hence, ELM mitigation techniques must be capable of reducing the ELM size by a factor of 20 relative to the unmitigated size [6].

In addition to the main consideration of mitigating the ELM heat load issue, these techniques must also be compatible with the overall energy confinement requirements of ITER required to achieve acceptable fusion gain Q. Transport simulations indicate that the attainable Q in ITER will be extremely sensitive to the temperature (or equivalently the pressure at a given density) just inside the edge transport barrier region. For a fixed width of the edge transport barrier, this sensitivity places a lower limit on the practical edge pressure gradient for successful $Q = 10$ operation in ITER. Because of the sensitivity of fusion power production to plasma density, it is essential that a technique be compatible with high density operation. The $Q = 10$ operating point for ITER is at an average density of 10^{20} m^{-3} (or 85% of the Greenwald density). Depending on the degree of density peaking that is present in a given regime, this requirement places a lower limit on the pedestal density that can be tolerated for $Q = 10$ operation. In contrast, an ELM mitigation technique must provide a sufficient level of impurity transport across the H-mode barrier to mimic the role of ELMs in contolling impurities during typical H-mode operation. The technique must also be compatible with the capabilities anticipated for ITER and compatible with other requirements of the scenario (e.g., stability, heat flux control, helium exhaust, etc.).

3 ELM CONTROL TECHNIQUES

Both stability and transport dynamics play important roles in the size and frequency of ELMs. The transition from L-mode to H-mode is coincident with the formation of a very strong edge transport barrier. The reduced power and particle transport through this region causes a rapid increase in the both the edge density and temperature gradients. On a longer time scale (the resistive time scale), the edge current density increases due to the pressure-gradient-driven bootstrap current. Eventually, the pressure gradient and edge current density become large enough that an ELM is triggered. Extensive research indicates that peeling-ballooning (P-B) stability theory describes the onset of ELMs [5]. A conceptual stability diagram described by peeling-ballooning theory is shown in Fig. 1. The stability boundary is dependent on both the edge pressure gradient (x-axis) and the edge current density (y-axis). The upper boundary of the stable regime is set by stability to peeling instabilities of low toroidal mode number (typically $n < 10$), which are very sensitive to the current density in the edge plasma. The right-hand boundary is defined by stability to ballooning-like instabilities and is hence very sensitive to the edge pressure gradient. Because of the near linear dependence of the bootstrap current on pressure gradient, operating trajectories typically traverse this diagram on a diagonal towards the upper right with a slope that is determined by the plasma collisionality.

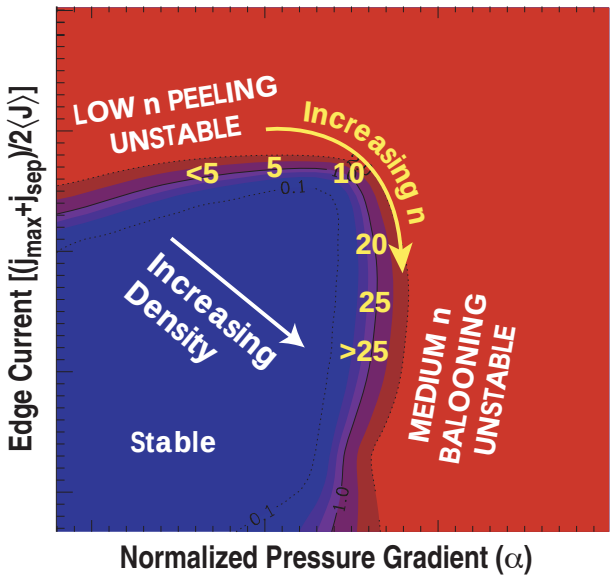

Fig. 1. Conceptual stability diagram for peeling-ballooning instabilities as a function of average edge curent density and normalized pressure gradient. The numbers at the instability boundary indicate the most unstable toroidal mode number.

In present-day devices, the largest Type I ELMs ($\Delta W_{ELM}/W_{ped} \simeq 10\%$) are typically observed when the pressure gradient and edge current density are large enough that the stability boundary is encountered in the upper right hand corner of this diagram. In this region, P-B theory predicts that the most unstable modes are coupled P-B modes with relatively large spatial extent. The exact location at which the operating point encounters the stability boundary is governed primarily by the efficiency by which bootstrap current is produced by the pressure gradient. This efficiency is most sensitive to changes in the collisionality of the edge plasma with lower collisionality plasmas having the largest bootstrap current. The upper right hand corner of Fig. 1 is generally associated with moderate to low collisionality, the condition expected in ITER.

3.1 Small ELM and ELM-free regimes

Many small ELM or ELM-free regimes have been developed and characterized [8]. These regimes generally incorporate one of three basic techniques for modifying the edge instablity threshold: 1) modification of the P-B stability boundary via plasma shaping or edge safety factor; 2) modification of the operating point on the P-B diagram; or 3) increased edge transport so that the operating point does not encounter the P-B stability boundary.

The P-B stability diagram is to the lowest order determined by the plasma magnetic geometry (i.e, the shape of the outer closed flux surfaces). Experimental studies have shown that changing the plasma shape robustly changes the ELM character (both in size and frequency). For example, changes in both the plasma triangularity and squareness can have a large impact on ELM size and frequency [9]. However, the reduced ELM size is generally accompanied by a reduction in the maximum pressure that can be obtained just inside the edge transport barrier, leading to reduced core energy confinement — an unacceptable consequence for ITER.

Increasing collisionality reduces the current drive efficiency, moving the intersection with the P-B threshold to the right side of Fig. 1, where the most unstable modes have smaller spatial extent. Consistent with the description above, increased collisionality is observed to generally lead to reduced ELM size (Fig. 3 in Ref. [10]). While only moderate loss of pedestal pressure and associated core confinement is generally observed for higher collisionality ELMs, such collisionality levels will likely not be accessible in ITER.

Of the many small and ELM-free regimes, only a few regimes have been realized at the anticipated collisionality of ITER: Type II ELMs, so-called grassy ELMs, and quiescent H-mode (QH-mode). The grassy ELM regime (originally observed on JT-60U) combines good pedestal characteristics with small ELMs at collisionality values ($\nu_e^* = 0.2 - 0.8$) consistent with ITER [11]. This regime is characterized by high frequency periodic edge instabilities of $800 - 1500$ Hz, which is ~15-30 times faster than that for Type I ELMs, yielding peak divertor heat flux reduced by a factor of 10 [12]. Grassy ELMs have been shown to be compatible with good confinement, internal transport barriers, and high pressure operation. However, access to this regime has been limited to operation at edge safety factor $q_{95} > 4$ (ITER's design point is $q_{95} = 3$), high $\beta_p \geq 1.6$ (defined as the ratio of the plasma pressure to the polodial magnetic field pressure), and very high triangularity $\langle\delta\rangle = 0.6$ ($\langle\delta_{ITER}\rangle = 0.45$). Because of the uncertainties in producing these conditions on ITER, it is unknown whether this regime can be achieved on ITER, especially at $q_{95} = 3$.

The QH-mode regime, originally developed on DIII-D, is characterized by a continuous MHD mode in the edge that increases the edge transport, enabling operation close to but slightly below the P-B stability threshold [13]. This regime has been achieved over a wide range of operating conditions (collisionality $= 0.04 - 0.3$) and plasma shapes and has good confinement and density control properties. To date, the regime has only been achieved in cases that have a large amount of applied torque in the toroidal direction. Stationary operation for extended duration has been achieved on several devices using counter neutral beam injection (NBI) (injection direction opposite to plasma current). More recent experiments on DIII-D have demonstrated the capability to access the QH-mode with strong co-NBI, albeit for limited duration [14]. Theory suggests that key elements for QH-mode access are low collisionality and high rotational shear in the edge region [15]. While low collisionality operation is expected in ITER, the ability to realize high rotational shear in ITER is uncertain due to the minimal torque delivery capabilities presently planned; hence, the ability to realize this regime on ITER is uncertain.

3.2 Triggering ELMs

The ELM cycle is characterized by a rapid loss of both the pressure gradient and current density in the edge region, followed by rebuilding of the edge transport barrier, edge pressure gradient, and ultimately the edge current density. The frequency of ELMs is therefore determined by the size of the

original ELM crash, the time for reestablishing the edge transport barrier, the time for the power flow through the edge to rebuild the edge pressure gradient, and the resistive diffusion time for the edge current density associated with the change in bootstrap current. Typical Type I ELM frequencies f_{ELM} for the "natural" ELM cycle on present-day devices range from $1 - 200\,\mathrm{Hz}$.

The instability boundary described by Fig. 1 is very sensitive to local conditions and can change dramaticially due to changes in edge parameters. Hence, small perturbations that modify the edge plasma appropriately can lead to the destabilization of ELMs. Controlled, periodic perturbations of this type could then be used to increase the ELM frequency relative to the "natural" ELM frequency. Studies have shown that the time-average energy loss due to ELMs in a variety of devices is roughly 20% of the input power (i.e., $\Delta W_{ELM} f_{ELM} = 0.2 P_{heat}$) [16]. Hence, if this scaling can be maintained at higher ELM frequency, the ELM size can be reduced by simply increasing f_{ELM}. Note that the ELM size reduction required for ITER ($\Delta W_{ELM}^{desired} / \Delta W_{ELM}^{natural} = 1/20$) requires that $f_{ELM}^{desired} / f_{ELM}^{natural} = 20$, is a key consideration for ELM triggering techniques in ITER.

Various techniques have been developed for triggering smaller Type I ELMs. Slowly ramping the plasma current (i.e., adding local current at the edge of the plasma) has been shown to increase f_{ELM} [17]. Periodic perturbations of the edge plasma using pellet injection or rapid vertical movements of the plasma have been used to regularly trigger ELMs and thereby control the ELM size. Details of ELM pacing by pellet injection will be discussed in Section 4.1.

The use of rapid vertical movements of the plasma was originally developed on TCV [18] and reproduced on ASDEX-Upgrade [19] and JET [20]. These studies indicate that a vertical movement of a few cm at frequencies above 50 Hz reliably trigger ELMs. The exact mechanism that leads to the destabilization of ELMs has not been identified though it is believed to be due to the modification of the current density profile very near the plasma edge. While vertical movements of the plasma of $\sim 5\,\mathrm{cm}$ at 20 Hz should be possible on ITER, the compatiblity with $n = 0$ vertical stability and A/C losses in the superconducting coils associated with this movement pose some concern.

3.3 ELM control through edge transport control

The continuous build-up of the edge pressure gradient and associated current density that leads to an ELM is due to the energy and particle flow across

the edge region being smaller than the input energy and particle flow to the plasma (or equivalently the flows from the core region to the edge). In some cases, the transport levels across this region (known as the edge transport barrier) approach zero, particularly for particles. In such a case, an instability is inevitable as the pressure gradient will build until the magnetic field pressure is unable to maintain force balance.

Hence, a means to avoid ELMs is to regulate transport across the edge transport barrier such that the edge pressure gradient can be maintained at a level just below the ELM instabilily limit. Unfortunately, because the exact mechanisms governing transport in this region are still unknown, a first principles approach to increasing transport in this region is presently not possible. However, there are many empirical examples in which such a transport state has been established and ELMs avoided. Operating regimes such as the Enhanced D-alpha (EDA) regime on Alcator C-Mod [21], the Type II ELM regime [22], and the aforementioned QH-mode regime in DIII-D have achieved quasi-steady-state edge conditions without large Type I ELMs. In each case, the increased edge transport is correlated with the presence of coherent instabilities that appear to be responsible for the increased edge transport. A detailed physics description of these instabilities is still lacking; hence, extrapolation to ITER is presently difficult.

The ability of these instabilities to drive substantial particle and energy flow across the region suggests another possibility for edge transport control: modifying the 2-D symmetry of the edge region by applying localized 3-D magnetic fields. When a 3-D field is applied that has a helical pitch similar (known as a resonant field) to the natural 2-D toroidally symmetric field, large displacements in the magnetic field trajectory can occur for small values of the applied 3-D field. In such a case, the applied 3-D fields increase the radial excursion of particles when traversing their particle orbits, thereby effectively increasing the radial transport of these particles.

The use of 3-D fields for edge control has been explored for several decades with the primary work performed on limiter devices ([23–26]) and TEXTOR. In all these cases, increased edge transport was observed with edge particle transport typically affected more than energy transport. More recent work has successfully extended these results to tokamaks using $n = 3$ RMPs, leading to complete suppression of ELMs. More details of these results and the implications for ITER are discussed in Section 4.2.

4 ELM CONTROL IN ITER

The present ITER baseline incorporates two systems for ELM control: ELM pacing using pellet injection and ELM suppression using RMPs at the plasma edge. While the physics basis of these techniques is still being developed, several physics requirements leading to engineering requirements for ITER have been identified and are described in this section.

4.1 ELM pacing using pellet injection

The triggering of ELMs using pellet injection has been observed on several devices ([27,28]). Subsequent research on ASDEX-Upgrade has shown the efficacy of using pellet injection at frequencies higher than the natural ELM frequency to increase the ELM frequency and reduce the ELM size (Fig. 2) [29]. These studies have shown that the ELM frequency can be locked to the pellet injection frequency up to a factor of 2 above the natural ELM frequency [Fig. 3(a)]. The concomintant plasma fueling associated with the pellet injection has been shown to have a modest effect on plasma confinement with $\tau_E \propto f_{ELM}^{-0.16}$ over a range of $20 - 80\,\mathrm{Hz}$. Note, however, that even this seemingly weak dependence with ELM frequency would have a significant effect in ITER since $f_{ELM}^{desired}/f_{ELM}^{natural} = 20$ would result in a 35% reduction in energy confinement according to this scaling.

This result suggests a key issue for ELM pacing in ITER to minimize overfueling of the plasma while still maintaining robust ELM triggering. Up to a certain throughput, fueling associated with pellet ELM pacing can be used to supplement fueling via the main pellet injector on ITER. However, very high fueling requirements for ELM pacing (e.g., large pellets at high frequency) are likely to have adverse effects on density control and plasma confinement. Therefore, the optimal pellet size should be sufficiently large (both in terms of penetration and perturbation) to robustly trigger ELMs but small enough that core fueling and convective losses due to the pellets are acceptable.

Research is now focusing on the penetration and perturbation size requirements for triggering the ELM robustly. Studies on ASDEX-Upgrade indicate that the pellet must penetrate to the inner side of the edge region (referred to as the top of the pedestal) to achieve 100% reliability that the pellet will trigger an ELM [Fig. 3(b)] [30]. Similar studies on DIII-D (albeit with a much

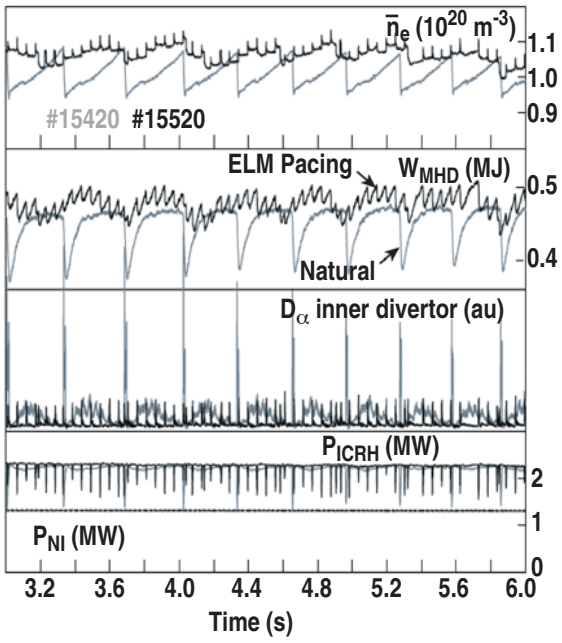

Fig. 2. Comparison of (a) density, (b), stored energy, (c) divertor recycling, and (d) power input sources for a case with repetitive pelling injection for ELM pacing and a comparison discharge with sufficient gas injection to match the average density as the ELM pacing case.

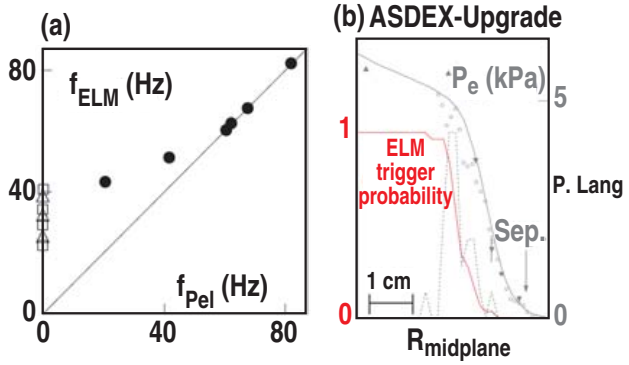

Fig. 3. ASDEX-Upgrade results of the (a) observed ELM frequency versus pellet injection frequency and (b) probability of triggering an ELM frequency versus pellet penetration depth.

smaller data set) suggest that pellet penetration half way through the edge region may be sufficient for robust ELM triggering. Work is in progress to reconcile these results in hopes of determining the minimum perturbation size required for reliable triggering of the ELM. While theories have been put forth to explain the mechanism through which a pellet triggers an ELM, detailed comparisons of these theories with experimental results are still needed.

The penetration requirements alone imply certain requirements on the pellet delivery systems in ITER. The established scaling for pellet penetration developed from a multi-machine database has the form [31]:

$$\lambda/a = C T_e^{-5/9} n_e^{-1/9} m_{pel}^{5/27} v_{pel}^{1/3} \quad , \tag{1}$$

where T_e is the electron temperature, n_e is the electron density, m_{pel} is the pellet mass, v_{pel} is the pellet velocity. For a fixed plasma condition at the edge (i.e., n_e and T_e fixed), the pellet penetration depth is dependent on both the pellet mass and velocity. For a chosen penetration requirement for robust ELM triggering (assumed presently to be the top of the pedestal), this coupled dependency means that the perturbation size (and its effect on plasma confinement and density control) and pellet velocity are integrally linked since $m_{pel} \propto v_{pel}^{-1.8}$. This coupling, shown graphically in Fig. 4 for three different assumptions of the edge density and temperature, poses several issues for implementation of this technique in ITER. It is important to note that the curves in Fig. 4 represent a minimal mass required for penetration to the top of the pedestal. Because the minimum perturbation size to robustly trigger ELMs is presently unknown, the mass required for pellet ELM pacing may be slightly larger than that required simply for pellet penetration. Note even larger pellets than this can be utilized, provided the overall fueling is compatible with the density control and plasma confinement requirements of ITER.

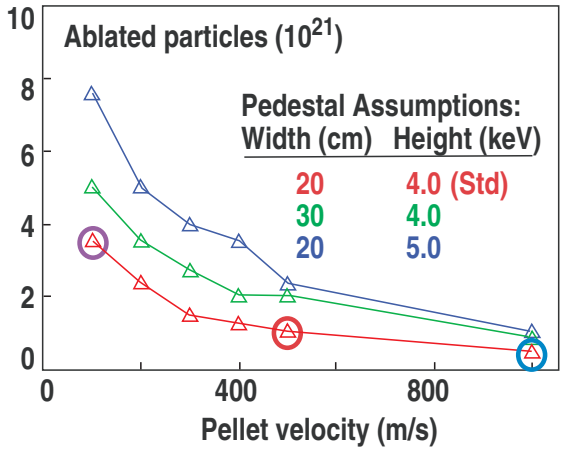

Fig. 4. Required pellet ablated mass versus pellet injection velocity for pellets penetrating to the top of the pedestal in ITER for various pedestal conditions.

Because the minimum perturbation size to robustly trigger ELMs is presently unknown, one can only address the relative tradeoff between pellet mass and velocity at present. In this regard, it is illustrative to explore the issues related

to three choices of potential pellet velocities that span the range of technical capabilities for ITER: 100 m/s, 500 m/s and 1 km/s. The fueling rate and estimated convective energy losses due to the rapid expulsion of the pellet mass from the plasma are tabulated in Table I. At $v_{pel} = 100$ m/s, the required pellet mass will result in plasma fueling rates that exceed the D-T burn rate by a factor of 80 and large estimated convective losses. Energy confinement and density control would undoubtedly be adversely affected. In addition, technology development would be required to develop the hardware that can robustly delivery 100 m/s pellets of the required size. By increasing the pellet velocity to 500 m/s, the fueling rate and estimated convective losses are reduced substantially, resulting in significant reductions in the impact on plasma confinement and density control. The technology is in hand to deliver pellets with this velocity and size. The use of 1 km/s pellets would reduce the fueling rate to near negligible levels with very small impact of plasma confinement and density control capabilities and would, therefore, be favored from an overall plasma impact point-of-view. Furthermore, the higher speed pellets will require a new launch configuration on ITER as pellets at this velocity have a very high probability of shattering in a curved pellet guide tube, which is incorporated in the present design for both fueling and ELM-pacing pellet injection on ITER.

In addition to the considerations on pellet mass and velocity discussed above, achieving the necessary perturbation without overfueling the plasma also favors injection from the low-field side to take advantage of the experimentally observed outward drift of ablated material. The high frequency that will be required in ITER ($>20-40$ Hz) will likely require multiple injectors for robust, reliable operation. Each of these injectors will need to have efficient propellant gas control to minimize the dilution impact on the core plasma. While there are still some physics and technology issues to be addressed, pellet ELM pacing on ITER appears to be feasible as well as compatible with other requirements of the operating scenario (e.g., density and impurity control), provided the required pellet size does not result in plasma overfueling.

Table I. Comparison of Estimated Parameters for Various Pellet Velocities in ITER

Pellet velocity (m/s)	100	500	1000
Fueling rate (10^{21} D/s)	140	40	4
Est. conv. loss (MW)	200	60	6

5 ELM MITIGATION USING RESONANT MAGNETIC PERTURBATIONS

Complete ELM suppression over a wide range of plasma shapes and edge conditions has been demonstrated in recent experiments on DIII-D [32] . These experiments utilize the unique capability of DIII-D to apply $n = 3$ (n is the toroidal mode number) magnetic fields of small amplitude ($10^{-4}B_T$) from a set of coils (known as the I-coils) located on the inner wall of the DIII-D vacuum vessel. The geometry of these coils along with a set of coils (known as the C-coils) outside the toroidal field coil cage are shown in Fig. 5. An example of a discharge in which ELMs have been completely suppressed is shown in Fig. 6.

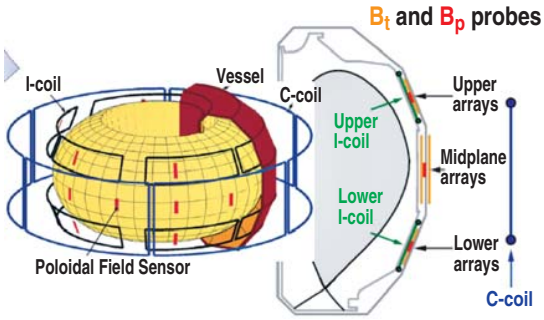

Fig. 5. Geometry of the internal I-coils and external C-coils in DIII-D.

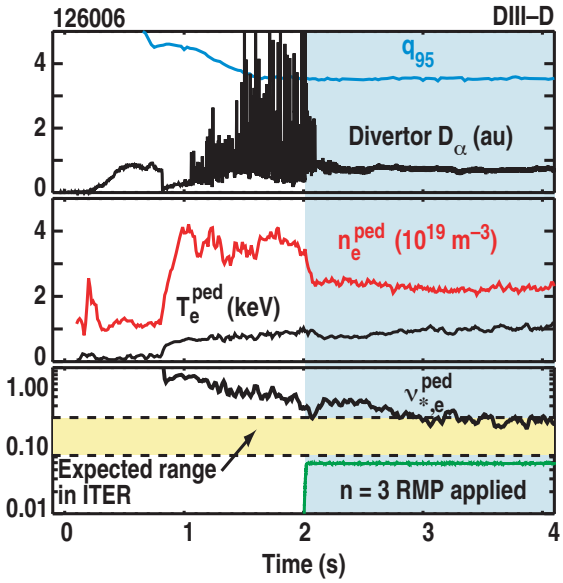

Fig. 6. Temporal evolution of a discharge in DIII-D in which the application of a $n = 3$ field after 3 s leads to ELM suppression.

In this case, vacuum field calculations indicate that the applied fields have a large amplitude of resonant fields in the edge region. This is illustrated in Fig. 7 where the amplitude of applied $n = 3$ field is shown versus poloidal mode number (m) and radial coordinate (ψ_N). The dashed magenta line represents the local pitch of the equilibrium magnetic field (i.e., where $nq = m$ where q is the plasma safety factor). At the edge of the plasma ($\psi_N \sim 0.9$), the field amplitudes are large along the path of $nq = m$, indicating a large resonant component at the edge. The amplitude of this resonant component decreases continuously as the distance inside the plasma edge increases. Note that because of the limitations of the present coil set on DIII-D, there are also large non-resonant (i.e., $nq <> m$) fields throughout the edge and core region. The implications of the core resonant fields and non-resonant fields will be discussed later in this section.

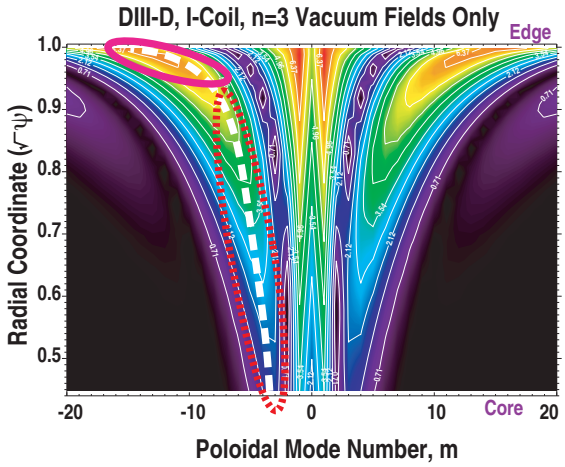

Fig. 7. Amplitude of the applied $n = 3$ field versus normalized flux and poloidal mode number for the case shown in Fig. 6. Scale (G): red: 7 ; yellow: 5.6; green: 4.2: cyan: 2.8, dark blue: 1.4, black: 0.

If realized in the plasma, the large displacement of the magnetic field lines at surfaces where $nq = m$ lead to the formation of magnetic islands. In the case shown in Fig. 7, this is most prevalent at the plasma edge. Increasing the field causes the radial extent of the island to increase. If the size of adjacent islands exceeds the width between the islands, then the magnetic field structure becomes stochastic. A measure of this stochasticity is the Chirikov parameter ξ_{Chir} defined as the ratio of island size to the width between islands. Theory suggests that when ξ_{Chir} exceeds unity, the magnetic topology is stochastic with adjacent field lines potentially having radically different trajectories, thereby enhancing cross-field transport. Studies on DIII-D have shown that there is a strong correlation between ELM mitigation/suppression

and the width over which $\xi_{Chir} > 1$ in the edge, shown in Fig. 8 [33]. Separate experimental observations, including the sensitivity of ELM suppression to the edge safety factor and the applied field spectrum, support the notion that island overlap and edge stochasticity play an important role in achieving ELM suppression [34]. Based on these results, the present design criteria for evaluation of ELM control coils for ITER is that the minimum width of the region with $\xi_{Chir} > 1$ should be approximately 8% of the plasma minor radius (or equivalently 15% in normalized flux) [6].

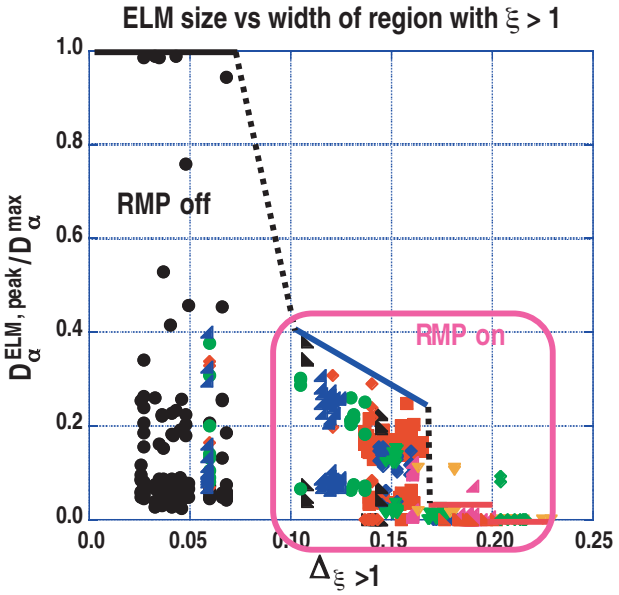

Fig. 8. Relative ELM size as measured by D_α perturbation relative to unmitigated ELM size versus computed Chirikov parameter (defined in text) for a series of discharges with different RMP perturbation amplitudes on DIII-D.

While this criteria focuses on ELM suppression specifically, there are several other considerations in choosing the best coil set for ITER. Primary among these is generating the required resonant field perturbation at the edge in ITER while minimizing "stray" resonant and non-resonant fields in the remainder of the plasma region. There are three design parameters to consider: the location and geometry of the coils as well as the current distribution in the coils. A key consideration in the design must be the ability to achieve ELM control over a range of operating conditions, including significant changes in the edge safety factor.

In vacuum, the applied fields are expected to decrease from their source as $\delta B_m \propto r^{-m}$. Hence, the ratio of the amplitude of the field in the core δB_o to that in the edge δB_{edge} required for achieving a specific δB_{edge} scales approximately as $\delta B_o/\delta B_{edge} = (1 - a_{plasma}/a_{coil})^m$ where a_{plasma} and a_{coil} are the

minor radius of the plasma and the coil, respectively. Hence, placing the coil as close to the plasma edge as possible is highly advantageous in localizing the perturbation to the edge plasma. This is particularly true for lower m fields in which the falloff in the field with distance from the coil is moderate.

As described earlier in the case of DIII-D, even with coils inside the vacuum vessel and close to the plasma ($a_{plasma}/a_{coil} \approx 1.4$), the application of resonant fields in the plasma edge leads to resonant fields in the core region and non-resonant fields throughout the plasma volume. If large enough, resonant fields in the core could lead to the formation of magnetic islands in the core region, reducing overall energy confinement and potentially providing seed islands for formation of neoclassical tearing modes. Conventional thinking is that non-resonant fields will adversely affect plasma rotation due to an applied torque of the form: $\eta_{NRMF} \propto -\Sigma\delta B_{mn}^2 V_\phi$ where δB_{mn} is the amplitude of the non-resonant field for m, n, and V_ϕ is the toroidal rotation. The reduced rotation associated with this torque is unfavorable for plasma confinement and increases the potential of locked modes leading to plasma disruptions. Recent experiments on DIII-D indicate that there is an offset velocity towards which the plasma decelerates/accelerates (i.e., $\eta_{NRMF} \propto -\Sigma\delta B_{mn}^2 (V_\phi - V_{offset})$ [35]. Depending on the initial velocity relative to offset velocity, the applied torque could result in an acceleration of the plasma. This is indeed observed in the experiment, which is consistent with the predictions of neoclassical torodial viscosity (NTV) theory [36], and may lead to a synergistic effect between the application of RMPs for ELM control in ITER and increased rotation and confinement.

To illustrate these tradeoffs, Fig. 9 compares the $n = 4$ field spectrum for three sets of coil designs that have been considered for ITER: 1) a single toroidal row of 18 coils at the outboard midplane; 2) two toroidal rows of nine coils above and below the outboard midplane; and 3) three toroidal rows of nine coils at, above, and below the midplane [37]. The coil currents in each case have been independently adjusted in order to achieve a width of $\xi_{Chir} > 1$ of 15% in normalized flux in the edge. As a result of this adjustment, all of the cases shown in Fig. 9 have comparable resonant field magnitudes at the plasma edge. However, the resonant fields in the core region and the non-resonant field amplitudes and structure are quite different. In the single row case [Fig. 9(a)], the pitch of the external coils is not well aligned with the plasma helicity and the peak of the applied spectrum is shifted towards lower m. To achieve the necessary field at $nq = m$ for island overlap, large non-resonant fields are produced throughout the plasma with potentially detrimental effects. With the addition of a second row of coils [Fig. 9(b)], the pitch of the applied field

can be well aligned with plasma helicity at $nq = m$. This leads to a significant reduction in the resonant fields in the core region and a large decrease in non-resonant fields over a large $\psi_N - m$ region. However, large non-resonant fields still are evident especially for $|m| < 5$ and along the contour of opposite field helicity ($nq = -m$). The presence of large fields with $|m| < 5$ is particularly worrisome due to the very slow falloff of these fields as they penetrate into the core. The addition of a third row [Fig. 9(c)] eliminates the non-resonant fields with $|m| < 5$ but the lobe at opposite helicity remains. This lobe is an unavoidable consequence related to the realizable coil geometries in the present ITER design. For future devices in which such a coil set could be included in the device design from conception, optimization of the coil set should be possible to significantly reduce or eliminate this unwanted lobe.

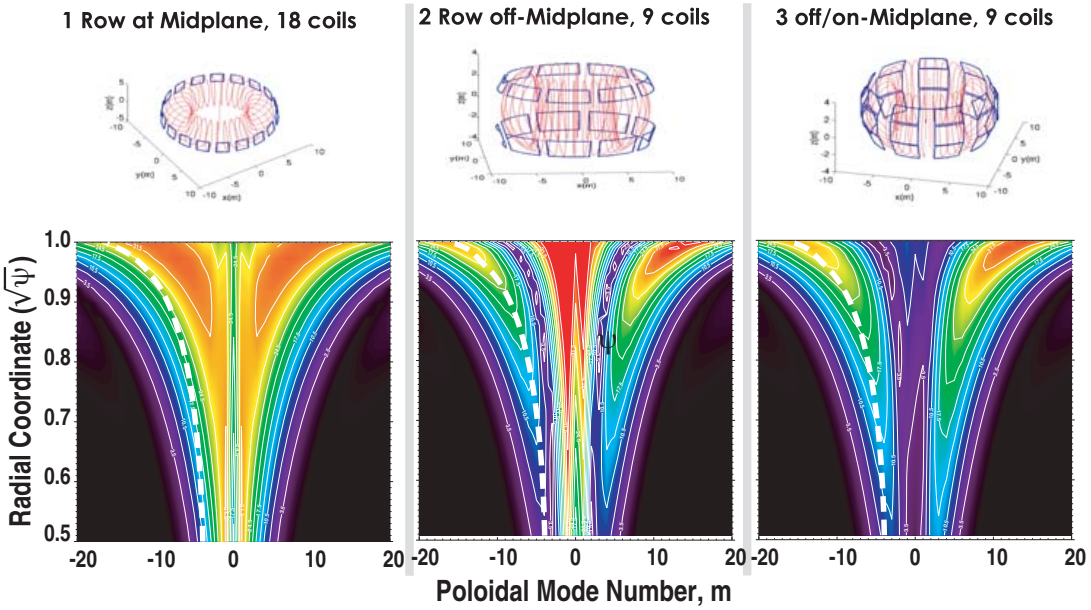

Fig. 9. Magnetic field spectra for three coil designs in ITER: (a) single toroidal row of 18 coils; (b) 2 toroidal rows of 9 coils above and below the midplane; and (c) 3 toroidal rows of 9 coils at, above, and below the midplane. Color scale is the same in all three cases. Scale (G): red: 35 ; yellow: 28; green: 21: cyan: 14, dark blue: 7, black: 0.

Note that Fig. 9 is based on calculations of vacuum fields alone. It is anticipated that the fields in the plasma will be quite different due to screening of the fields by plasma rotation or amplification of the fields by resonant plasma responses. While the physics basis of the plasma response to applied fields is still in development, recent studies have had some success in predicting the plasma response to applied or intrinsic non-axisymmetric fields. As an example, the Ideal Perturbed Equilibrium Code (IPEC) [38], which computes a 3-D perturbed equilibrium include plasma response effects such as poloidal

harmonic coupling, shielding, and amplification has been successfully used to explain the plasma sensitivity to error fields in NSTX and DIII-D [39]. This code has also been used to evaluate the plasma response to the applied fields from ELM control coils on ITER. The results, shown in Fig. 10, quantitatively confirm the qualitative analysis described above. In this case, the proxy for the effect on core plasma rotation is taken to be the drag from NTV theory, which is proportional to the $\Sigma\delta B_{mn}^2$. The optimized case (i.e., the 3-row case above) is seen to have reduced core drag relative to the 1-row case by two orders of magnitude. As exemplified by the "theoretical best" curve in Fig. 10, additional improvement would be possible if more flexibility in the coil design were possible

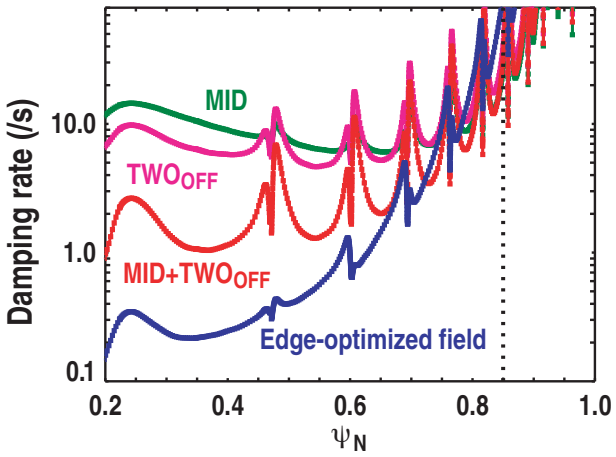

Fig. 10. Computed drag from NTV calculated by IPEC for three cases shown in Fig. 9 as well as a theoretically optimized case.

The above physics requirements imply specific engineering requirements for implementing ELM control coils in ITER. These requirements favor a coil set that is as close to the plasma as possible (preferably inside the vacuum vessel) that has multiple toroidal rows on the outboard midplane and the capability of applying perturbations of a range of low n toroidal mode numbers. This coil set must be capable of high current operation, implying a multi-turn design that is actively cooled. Because of the proximity of the coil set to the plasma, shielding of these coils will be minimal, implying the use of ceramics for insulation of these coils. In addition, these coils must be highly reliable at their full-field specification as a single large ELM has the potential of eroding/melting significant plasma facing surface material in ITER.

In addition to these engineering issues, there are still several unresolved physics issues for RMP control of ELMs. Primary amongst these is the observation of a large density reduction in many DIII-D cases. Such a large density reduction

in ITER would have far-reaching implications on the compatibility of RMP ELM suppression with $Q = 10$ operation. The degreee of density decrease varies signficantly in DIII-D studies, ranging from 8%-40%. Because of this large range, it is difficult to assess the impact of the density decrease on ITER operation. More detailed experimental and theoretical studies are needed to determine the underlying cause of the density loss. The fundamental compatibility of RMP ELM suppresion with pellet injection for density control has been demonstrated with a small number of pellets in series; tests with an extended series of pellets are still needed. Although initial studies with the RMP showed significant impurity accumulation, more recent studies in which the interaction of the divertor plasma with the material surfaces is better controlled have shown the compatibility of operation with $Z_{eff} < 2$ during RMP ELM suppresion [34].

6 SUMMARY

The critical nature of ELM control in ITER operations is exemplified by the ITER design incorporating two independent control tools for ELM control: ELM pacing using repetitive pellet injection and ELM suppression using RMPs from a set of in-vessel coils. While the physics requirements for each technique are still being refined, the gross features of the hardware required for ELM control in ITER can be defined. For ELM pacing by pellets, moderate-speed, moderate-mass pellets launched from the outboard midplane at a rate of 20 Hz with efficient propellant control will be required. The choice in the tradeoff between pellet velocity and size is constrained by the minimum pellet mass required for ELM triggering and the range of pellet velocities that can be reliably achieved. The physics requirements for RMP ELM control imply specific constraints on the location, geometry, and current distribution of the coils. Locating the RMP coils inside the vacuum vessel is highly favored in order to minimize the penetration of fields further into the plasma. Multiple toroidal rows of coils would maximize the edge resonant perturbation while minimizing resonant and non-resonant fields. The current distribution in the coils can be utilized to vary the toroidal mode number of the applied spectrum, which will be needed for ELM control over the full range of ITER operating space. While research is still needed to improve the physics basis of these ELM control techniques, the research to date has provided key information on the engineering requirements of these systems for successful implementation in ITER.

References

[1] Editors of Progress in ITER Physics Basis, Nucl. Fusion **47** (2007) S1.

[2] H. Zohm, Plasma Phys. Control. Fusion **(**38) (1996) 1213.

[3] D. Hill, J. Nucl. Mater. **241-243** (1997) 181.

[4] M. Becoulet, Plasma Phys. Control. Fusion **45** (2003) A93.

[5] P.B. Snyder *et al.*, Nucl. Fusion **44** (2004) 320.

[6] P. Thomas *et al.*, Proc. 22nd IAEA Fusion Energy Conference, Geneva (2008).

[7] J. Linke *et al.*, Proc. 13th Int. Conf. on Fusion Materials, Nice (2007).

[8] N. Oyama *et al.*, Plasma Phys. Control. Fusion **48** (2006) A171.

[9] J.R. Ferron *et al.*, Phys. Plasmas **7** (2000) 1976.

[10] A. Loarte *et al.*, J. Nucl. Mater. **313-316** (2003) 962.

[11] Y. Kamada *et al.*, Plasmas Phys. Control. Fusion **42** (2000) A247.

[12] N. Oyama *et al.*, Nucl. Fusion **45** (2005) 871.

[13] K.H. Burrell *et al.*, Phys. Plasmas **8** (2001) 2153.

[14] K.H. Burrell *et al.*, submitted to Phys. Rev. Lett. (2009).

[15] P.H. Snyder *et al.*, Nucl. Fusion **47** (2007) 961.

[16] A. Herrman *et al.*, Plasma Phys. Control. Fusion **44** (2002) 883.

[17] J. Lingertat *et al.*, J. Nucl. Mater. **266-269** (1999) 124.

[18] A. Degeling *et al.*, Plasma Phys. Control. Fusion **45** (2003) 1637.

[19] P. Lang *et al.*, Plasma Phys. Control. Fusion **46** (2004) l31.

[20] F. Sartori *et al.*, Proc. 35th EPS Conf. on Plasma Physics, Crete, Greece (2008).

[21] M. Greenwald *et al.*, Phys. Plasmas **6** (1999) 1943.

[22] J. Stober *et al.*, Nucl. Fuison **41** (2001) 1123.

[23] N. Ohyabu *et al.*, J. Nucl. Mater. **121** (1984) 363.

[24] P. Ghendrih *et al.*, Nucl. Fusion **41** (2001) 1401.

[25] K. Finken *et al.*, Contrib. Plasma Physics **56** (2006) 515.

[26] C. Pires *et al.*, Plasma Phys. Control. Fusion **47** (2005) 1609.

[27] P. Lang *et al.*, Nucl. Fusion **36** (1996) 1532.

[28] L.R. Baylor *et al.*, Phys. Plasmas **7** (2000) 878.

[29] P. Lang *et al.*, Nucl. Fusion **43** (2003) l110.

[30] P. Lang *et al.*, Nucl. Fusion **45** (2005) 502.

[31] L.R. Baylor *et al.*, Nucl. Fusion **37** (1997) 445.

[32] T.E. Evans *et al.*, Nucl. Fusion **48** (2008) 024002.

[33] M.E. Fenstermacher *et al.*, Phys. Plasmas **15** (2008) 056122.

[34] M.E. Fenstermacher *et al.*, Nucl. Fusion **48** (2008) 122001.

[35] A.M. Garofalo *et al.*, Phys. Rev. Lett. **101** (2008) 195005.

[36] A. Cole *et al.*, Phys. Rev. Lett. **99** (2007) 065001.

[37] M.J. Schaffer *et al.*, Nucl. Fusion **48** (2008) 024004.

[38] J.-K. Park *et al.*, Phys. Plasmas **14** (2007) 052110.

[39] J.-K. Park *et al.*, Phys. Rev. Lett. **99** (2007) 195003.

Acknowledgment

This work was supported by the US Department of Energy under DE-FC02-04ER54698. The research represented here is from a large number of experimentalists, theorists, modelers, and engineers. I would particularly like to acknowledge the contributions to this paper of L.R. Baylor, T.E. Evans, P. Lang, and M.J. Schaffer.